

Equilibrium and Kinetics Studies of the Adsorption of Basic Dyes onto PVOH Facilely Intercalated Kaolinite - A Comparative Study of Adsorption Efficiency

Chighbundu C. Emmanuel* and Adebowale O. Kayode

Received:29 September 2021/Accepted 23 November 2021/Publishedonline:15 December 2021

Abstract: Most basic dyes are known for their toxic impact on the environment, especially in the aquatic ecosystem. Unfortunately, consistent discharge of dye containing wastes into most water bodies has generated serious challenges, which can only be solved through consistent research approaches. This study is designed to compare the adsorption capacities of purified (PRK) and polyvinyl alcohol (PVOH) intercalated raw kaolinite (PIK) for the adsorption of some basic dyes from an aqueous solution. Scanning electron microscope (SEM) with energy dispersive X-ray (EDX), Fourier-transform infrared (FTIR) Spectroscopy and X-ray diffractometer (XRD) were used to verify changes in morphology, surface functional groups and crystal lattice sequence adjustment in PIK adsorbent. Cation Exchange Capacity (CEC) and Point of Zero Charge (PZC) of both adsorbents were determined by methylene blue adsorption and salt addition technique, respectively. The adsorption characteristics of both adsorbents were investigated under various conditions such as varying adsorbent dosages, period of contact, temperature and pH. Thermodynamic parameters were used to evaluate the effect of temperature on the adsorption process, while non-linear regressions were used to fit the experimental data to various adsorption and kinetic models. UV-visible spectrometer was used to determine the absorbance of dyes left in the solution un-adsorbed throughout the experimental study. The morphology of PIK revealed a compacted structure with pores, while the crystal lattice adjustment of PIK

showed basal plane contraction to 4.06Å when compared with PRK respectively. Surface functionality study revealed several peaks such as CH₃ and CH₂ assigned to 2893 and 2990 cm⁻¹ respectively on PIK but absent on the FTIR graph of PRK. The adsorption isotherm model showed that PIK was twice efficient for the uptake of BR2 and BG5 compared to PRK. The Elovich model equation suitably described the adsorption kinetics while the thermodynamic parameters revealed that the adsorption was spontaneous and endothermic. In comparison to other desorption agents, acetic acid was found to be a good desorption agent.

Keywords: Intercalation, polyvinyl alcohol, kaolinite, Basic dyes, adsorption equilibrium

Chighbundu C. Emmanuel*

Chemical and Food Sciences Department,
Bells University of Technology, Ota, Ogun
State, Nigeria.

Email: ecchighbundu@bellsuniversity.edu.ng

Orcid id: 0000-0002-3413-9188

Adebowale O. Kayode

Department of Chemistry, Faculty of Sciences,
University of Ibadan, Oyo State, Nigeria.

E-mail: koadebowale@mail.ui.edu.ng

1.0 Introduction

Kaolinite is a mineral (Al₂O₃·2SiO₂·2H₂O) whose crystal structure consists of silicon tetrahedral and aluminum octahedral sheets superimposed on each other (Abdullahiet al.,2017), The compound is abundantly available at relatively low cost in Nigeria. The

<https://journalcps.com/index.php/volumes>

Communication in Physical Science, 2021, 7(4): 331-347

mineral is partially charged and has been widely utilized in several applications including pharmaceutical (drug delivery) and cosmetics formulations (Carretero and Pozo, 2010; Tan *et al.*, 2015), heterogeneous catalysis (Herney *et al.*, 2010), the production of glossy papers and as additives for rubbers and other polymers (Dewiet *et al.*, 2018). The use of kaolinite and other clay minerals in the decontamination of harmful pathogens and other forms of water pollutants has also been extensively investigated (Xue *et al.*, 2012; Ma *et al.*, 2014; Unuabonahet *et al.*, 2018; Shabanet *et al.*, 2018; Kuanget *et al.*, 2020). However, the application of kaolinite in the adsorption removal of dyes from aqueous solutions has been affirmed by some researchers. For example, Das *et al.* (2020) found that kaolin is an excellent adsorbent for the uptake of annatto dye in an aqueous solution. The efficiency of the adsorption process was reported to be strongly dependent on the particle size of the adsorbent, agitation rate and other parameters. Calculated thermodynamic parameters supported favourable adsorption that was exothermic, spontaneous and ordered. The adsorption characteristics of kaolin for the removal of brilliant green dye from aqueous solution were investigated by Nandi *et al.* (2009). They reported the high efficiency of the clay materials for the adsorption removal of the dye from an aqueous solution and found that the removal efficiency was strongly dependent on pH and the surface area. Characterization of the adsorbent was done using BET, XRD and other instrumentation. In all cases, the adsorption was spontaneous, endothermic, diffusion-controlled and fitted the pseudo second-order kinetics. Sarma *et al.* (2019) have also reported better adsorption efficiency for acid treated kaolinite compared to the untreated kaolinite. The adsorbents were characterized using XRD, FTIR, SEM and results obtained from the batch adsorption experiments fitted the Langmuir adsorption isotherm and the pseudo-second-order kinetic model. The

impacts of dyes on the aquatic system have been extensively reviewed. Dyes can obstruct the photosynthesis process in phytoplankton by limiting light penetration (AL-Da,amyet *et al.*, 2013; Odoemelam *et al.*, 2018; Kuanget *et al.*, 2020). Most dyes are not biodegradable but can form stable complexes with metal ions in the water (Eddy *et al.*, 2004). Toxic impacts of dyes on aquatic life have been confirmed (Kuanget *et al.*, 2020; Sarmaet *et al.*, 2019;). Some of the techniques that have been adopted to remediate dye contaminated aquatic environment include biological methods (biodegradation), physical techniques (precipitation, filtration, membrane separation, etc), chemical methods (ozonation, oxidation, electro dialysis, coagulation) and others (Bahareh *et al.*, 2014; Unuabonahet *et al.*, 2018; Sarmaet *et al.*, 2019; Kuanget *et al.*, 2020). Some of these technologies are either not effective for dye removal or uneconomical (Kuanget *et al.*, 2020).

Application of the adsorption process for the removal of dye molecules from aqueous systems is one of the most efficient approaches (Omorogieet *et al.*, 2014; Ogboduet *et al.*, 2015; Rashid *et al.*, 2016). The effectiveness of some adsorbents can be significantly enhanced through surface modification (Mbayeet *et al.*, 2014; Ogboduet *et al.*, 2015; Tabak *et al.*, 2016; Sarmaet *et al.*, 2019; Kuanget *et al.*, 2020). Intercalation is a process of inserting molecules into the space of layered material such as the interlayer planes of clay minerals. Various approaches are useful in the achievement of formation of interlayer expansion but the guest-displacement reaction is one of the most practical methods (Mezianeet *et al.*, 2017), which involves the initial insertion of smaller sized chemicals (such as urea, DMSO, acetamide and formamide) as precursors for the initiation of an interlayer expansion (Letaief and Detellier 2008; Jinet *et al.*, 2010). (Gardolinskiet *et al.*, 1998; Mbeyet *et al.*, 2013; Zhang *et al.*, 2013; Makóet *et al.*, 2019). The present study aims to investigate the feasibility of facile and direct intercalation



of purified naturally sourced kaolinite with polyvinyl alcohol (PVOH) to produce different hybrids of adsorbent that explores the interlayer space of the clay and researches its efficiency for the uptake of Basic Red 2 (BR2) and Basic Green 5 (BG5) dyes from aqueous solution

2.0 Materials and methods

2.1. Materials

2.1.1. Adsorbate and Adsorbent

Pristine kaolinite was obtained from Delta State, Nigeria. Basic Red 2 (BR2) (Safranin-O) and Basic Green 5 (BG5) (Methylene green zinc chloride double salt) dyes were supplied by BDH Prolabs chemicals (Table 1). Polyvinyl alcohol (PVOH) was supplied by

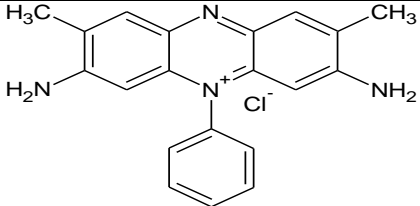
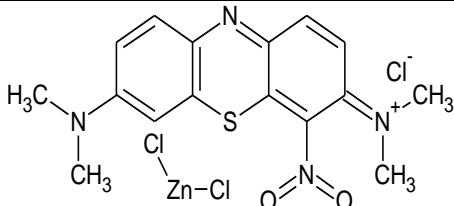
Sigma Aldrich Company, without being purified further both chemicals were utilized.

2.2 Methods

2.2.1. Purification of raw kaolinite

The pristine raw kaolinite clay material was dispersed in distilled deionized water, stirred and decanted until the colloidal clay materials were removed. The kaolinite was treated with a 30% hydrogen peroxide solution to oxidize any carbonaceous matter present (Yuan and Bish 2010). The product obtained was washed with distilled water to free hydrogen peroxide (IFRA 2019). Centrifugation was used to recover the peroxide-free kaolinite, which was subsequently oven-dried at 353 K and labeled PRK. (Purified Raw kaolinite).

Table 1 Molecular dimensions of the (Basic dyes) adsorbates

	Safranin Basic Red 2 (BR2)	Basic Green 5 (BG5) zinc chloride double salt
Molecular structure		
IUPAC name	3,7-dimethyl-10-phenylphenanzin-10-ium-2,8-diaminechloride	Dichlorozinc (7-(dimethylamino)-4-nitrophenothiazin-3-ylidene)-dimethylazanium chloride
Molecular formula	$C_{20}H_{19}N_4Cl$	$C_{16}H_{17}ClN_4O_2S \cdot 0.5ZnCl_2$
Molecular mass (g/mol)	350.85	501.10
Dye content	$\geq 85\%$	$\geq 80\%$
λ_{max} (nm)	520	663
Colour	Red	Green

Hazard Statements** *Skin corrosion/irritation (15.38%) Serious eye damage/eye irritation (80%) Inflammation of the respiratory tract (16.92%) Single-exposure toxicity to specifically targeted organs;*

2.2.2. Preparation of polyvinyl alcohol (PVOH) intercalation Kaolinite

Polyvinyl alcohol intercalated kaolinite was prepared using the method reported by Unuabonahet *al.*, (2008), with a slight

modification. 2 g of PVOH granule was dispersed in 300 ml of distilled deionized water and agitated while on a hot plate at a temperature of 333 K until a clear viscous solution was obtained. Afterward, 20 g of kaolinite was dispersed into the clear



viscous solution and swiftly agitated until kaolinite-gel was formed. The semisolid product was dried in an oven to constant weight at 333 K. A hardened dried sample was obtained which was gently crushed to smaller particles and sieved to achieve the desired fine particles labeled PIK (PVOH Intercalated Kaolinite) sample.

2.2.3. Characterization of the adsorbent

SHIMADZU Fourier Transform Infrared (FTIR) Spectrophotometer at a wavenumber range of 4000 – 350 cm⁻¹, resolution of 4 cm⁻¹ and Happ- Genzel apodization was used to analyze the functional groups on the surfaces of PRK and PIK sorbents. PhenonProX Scanning Electron Microscope (SEM) with EDX was employed to deduce the morphological surface characteristics of the sorbents. PHILIPS PW3040/60 X’Pert X-Ray Diffractometer was used to deduce the crystalline phase changes on the intercalated sorbent. The physicochemical characteristics of the adsorbents (PRK and PIK) were figured out via the determination of their Bulk densities (BD) (g/cm³), by the method used by Sousa *et al.*, (2013), Loss on ignition (LOI) (%) by the method used by Abella and Zimmer(2007), Point of zero charges (PZC) by Nwosuet *al.*, (2018), Methylene Blue Adsorption (MBA) surface area (m² g⁻¹) by Salwa and Essam, (2011) and Cation exchange capacity (CEC) (meq/100 g) by also the method adopted by Salwa

and Essam, (2011) while EDX-Carbon content (%), and particles size (µm) was determined by scanning electron microscope.

2.3. Adsorption experiment

2.3.1. Preliminary Experiments

The concentrations of the unadsorbed dye after each adsorption were determined from the absorbance characteristics of BR2 and BG5 dyes at λmax = 520 and 663 nm respectively using UV-vis spectrophotometer[Surgifriend SM7504UV/visible 911]. The adsorption capacity of the dyes was calculated using the following expression:

$$Q_e = \frac{(C_o - C_e)V}{m} \tag{1}$$

$$\% = \frac{(C_o - C_e) \times 100}{C_o} \tag{2}$$

where Qe is the quantity of dye adsorbed (mg/g), Co and Ce are the initial and equilibrium dye concentrations of the dye while V is the volume (L) of the solution and m is the mass (g) of the adsorbent used for the study.

Various operating conditions such as adsorbent dose, initial dye concentration, contact time and temperature were investigated using the methods described by Adebowale *et al.*, 2010.

Table 2 shows the non-linear forms of the different model equations employed to describe the adsorption and kinetic parameters.

Table 2: Some nonlinear adsorption and kinetic models

Model	Equation	Reference
Langmuir	$q_e = \frac{q_m K_L C_e}{1 + K_L C_e}$	Langmuir, 1918
Freundlich	$q_e = K_F C_e^{1/n}$	Freundlich, 1906
Redlich-Peterson	$q_e = \frac{K_R C_e}{1 + a_R C_e^g}$	Redlich and Peterson, 1959
Sips	$q_e = \frac{K_s C_e^{n_s}}{1 + a_s C_e^{n_s}}$	Sips, 1948
Fritz-Schluender	$q_e = \frac{A C_e^\alpha}{1 + B C_e^\beta}$	Fritz-Schluender, 1974
Pseudo-first order	$q_t = \frac{k_2 q_e^2 t}{1 + k_2 q_e t}$	Lagergren, 1898
Psuedo- second -order	$q_t = \frac{k_2 q_e^2 t}{1 + k_2 q_e t}$	Ho and Mckay, 1998



Elovich	$q_t = \frac{1}{\alpha} \ln(1 + \alpha\beta t)$	Low, 1960
----------------	---	-----------

2.4 Desorption Study

A mass of 0.08 g of the adsorbents was added to 100 mL of 50 mg/L of the dye solutions and shaken for 1 h. By centrifugation, the unadsorbed dyes were separated and the concentration was determined using UV- spectrophotometry. After which dye loaded adsorbents will be dried at 313K. Desorption study for the recovery of PRK and PIK adsorbents was carried out by mixing 0.5% of 0.02 M of H₂SO₄, HCl, CH₃COOH, NaCl and NaOH respectively and at an agitation time of 180 min for each (Bello *et al.*, 2008). The concentrations of the desorbed dyes (BR2 and BG5) were determined and desorption efficiency was calculated using the following expression:

$$\text{Desorption efficiency (\%)} = \frac{q_{des}}{q_{ads}} \times 100 \quad [6]$$

Where q_{des} and q_{ads} are quantities desorbed and adsorbed respectively.

3.0 Results and Discussion

3.1 Physicochemical characterization of adsorbents

The results presented in Table 3 are some of the outcomes obtained from the characterization of PRK and PIK. The Specific surface area (SSA) for PRK after adsorption of methylene blue (MBA) was 23.97 m²/g while that of PIK adsorbent was 19.33 m²/g. This confirms that surface modification occurred. The PZC of PRK and PIK samples were measured at pH values of 3.67 and 4.02 indicating that the modification of PRK with the polymer (PVOH) raised the PZC of the kaolinite clay sample (Fig. 1 and Table 3).

The cation exchanged capacity of PIK was observed to be 4.15 which is lesser compared to that of PRK calculated to be 7.65. This suggests that the polymer molecules have covered the surface of the kaolinite clay sample such that it has rendered the anionic sites on it inaccessible for enough cation exchanging reaction.

The cation exchanged capacity of PIK was observed to be 4.15 which is lesser compared to that of PRK calculated to be 7.65. This suggests that the polymer molecules have covered the surface of the

kaolinite clay sample such that it has rendered the anionic sites on it inaccessible for enough cation exchanging reaction.

Table 3 Adsorbent physicochemical characterization.

Parameters analyzed	PRK	PIK
Bulk density (g/cm³)	0.83	0.47
LOI (%)	4.31	13.56
PZC	3.67	4.02
Particles size (µm)	19.0-20.8	22.3-31.68
Surface area (m² g⁻¹)	23.97	19.33
CEC (meq/100 g)	7.65	4.15
EDX-(Carbon) (%)	1.2	1.9

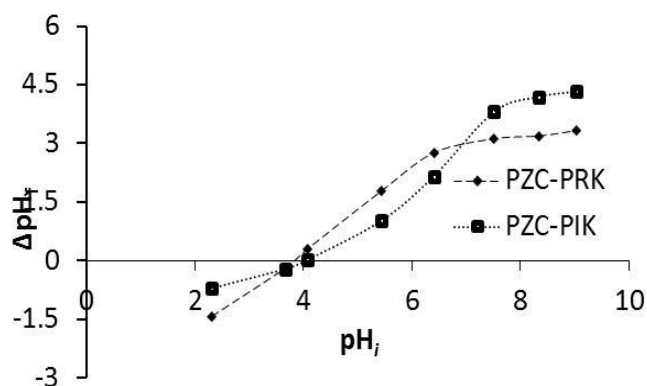


Fig.1. Point of zero charges.

The cation exchanged capacity of PIK was observed to be 4.15 which is lesser compared to that of PRK calculated to be 7.65. This suggests that the polymer molecules have covered the surface of the kaolinite clay sample such that it has rendered the anionic sites on it inaccessible for enough cation exchanging reaction.

3.2 Scanning Electron Microscopy (SEM) analysis

The micrographs of PRK and PIK are shown in Figs 2a and 2b respectively. The image of PRK showed grainy aggregation of particles with a mixture of triangular-like and hexagonal-like crystal structures (Fig. 2a). Uniformly dispersed arrays of small white patches are also observable which seem coarser and are likely to be silt and



sand in the clay. The observed, bright patches noticeable on the external surface of PRK micrograph, on one hand, is suggestive of open-end pores that can be useful for sorption purpose while on the other hand, other research worker has also observed similar micrograph for kaolinite and have suggested such deposits of white patches to consist of oxides of sodium, potassium, calcium, iron, magnesium, etc. (Sarma *et al.*, 2019). After the PRK sample modification process, the sample completely transformed into clumped compacted particles of PIK, lacking orderliness in their structure. In an actual sense, the PIK particles are more water-stable aggregates when left in water.

The percentage elemental emission for PRK before modification detected silicon (Si ~ 11.2%), aluminium (Al ~ 9.2%), oxygen (O ~ 77.2%), carbon (C ~ 1.2%), titanium (Ti ~ 0.5%) and iron (Fe ~ 0.7%) (Fig. 2a) while the EDX for PIK as shown in Fig. 2b revealed the percentage silicon (Si ~ 12.3%), aluminium (Al ~ 10.8%), oxygen (O ~ 81.3%), carbon (C ~ 14.2%).

3.3 Fourier Transformed Infrared Spectrophotometer (FTIR)

The FTIR spectra ranges (4000 – 350 cm^{-1}) for PRK and PIK are stacked for comparison and shown in figure 3.

Two strong bands at 3695 and 3652 cm^{-1} on PRK spectra are kaolinite characteristic band assigned to -O-H stretch vibrations, 1033 cm^{-1} , and 1008 cm^{-1} are attributed to -Si-O-Si and Si-O-Al bending vibration (Caponi *et al.*, 2017) The peaks for Si-O, Si-O-Si, Al-O-Si, and Al-Al-OH bending vibrations observed around 798 cm^{-1} , 694 cm^{-1} , 538 cm^{-1} and 470 cm^{-1} respectively also confirmed that the clay is more of kaolinite in terms of purification (Saikia and Parthasarathy, 2010). 3620 cm^{-1} is attributed to -OH stretching of inner hydroxyl which also agrees with the peaks at 910, 914 and 936 cm^{-1} for -OH deformation of inner-surface hydroxyl of (Al-Al-OH) according to Zsirka *et al.* (2015), Bands at 1795 and 1629 cm^{-1} falls within the range for the bending vibrations of water molecules (H-O-H) (Nwosuet *et al.*, 2018). Additional peaks at 701 cm^{-1} and 755 cm^{-1} are associated with the surface hydroxyls the same as reported by Djomgoue and Njopwouo, (2013).

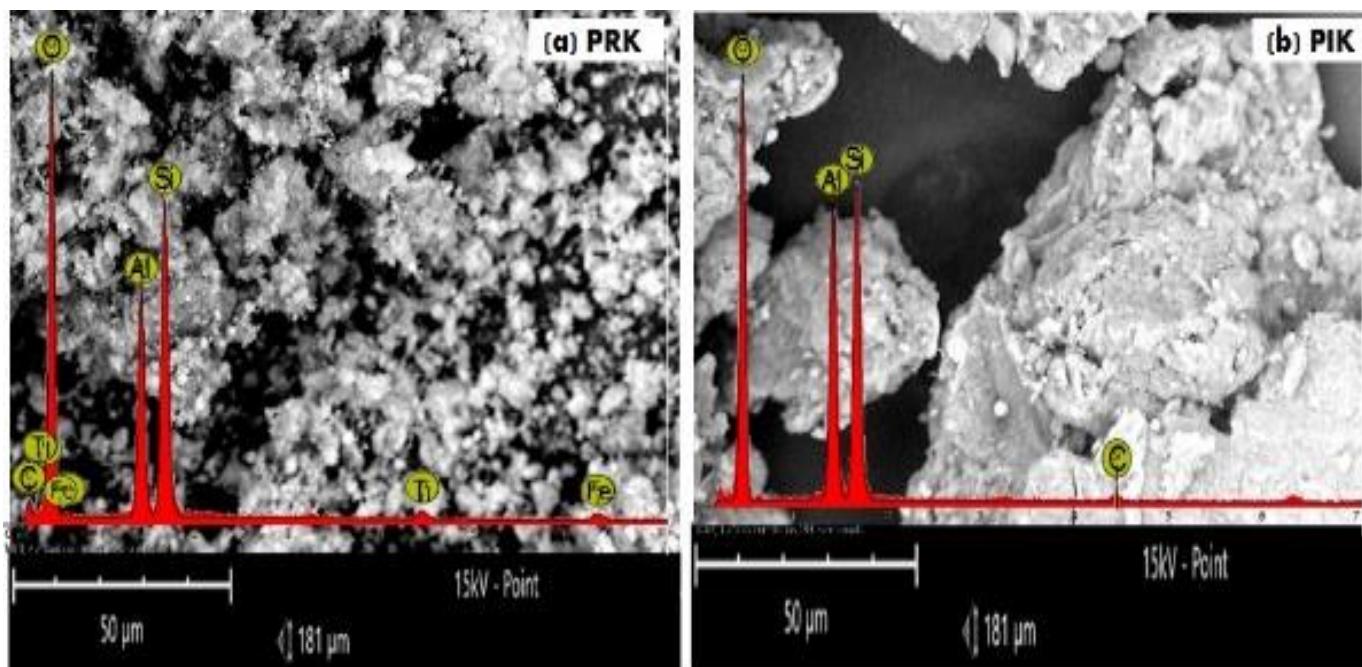


Fig. 2: Scanning electron microphotographs with their respective EDX of (a) PRK and (b) PIK

Fig. 3 shows the surface functionality of PIK, the characteristic band of O-H stretching vibration band of PVOH around 3000-3700 cm^{-1} is closer to

the peaks reported by El-Latif *et al.*, (2010) corresponding to -OH of alcoholic groups. Bands at 2945 and 2909 cm^{-1} , were assigned to methyl (-



CH₃) and methylene (-CH₂) symmetric and asymmetric vibrations respectively (Jung *et al.*, 2018). The appearance of broadband around 3283-3302 cm⁻¹ assign to hydroxyl group according to Alkan and Benlikaya(2009) arose due to the strengthening of hydrogen bonds between silanol (-SiOH) groups on the surface of PIK. The characteristic hydrogen-bonded carbonyl, (C=O) band which was suggested to appear at 1710 cm⁻¹ by Alkan and Benlikaya (2009), was observed to appear on the PIK spectrum at 1797 cm⁻¹. The band at 1629 cm⁻¹ (Fig. 3) which was assigned to O-H bending vibration of H₂O on PRK spectra was discovered to have shifted to a peak around 1633 cm⁻¹ in PIK spectra with a lower intensity which is an indication that there was an interlayer plane distortion.

3.4 X-Ray Diffractometry (XRD)

The XRD patterns of PRK and PIK samples (Figure not shown) revealed different arrangements of the kaolinite layers before and after the insertion of PVOH molecules in the interlayers. The XRD pattern of PRK revealed peaks of different relative intensities (Figure not shown) at $2\theta^0 = 12.35^0$, 19.79^0 , 20.84^0 and 24.85^0 with the crystal plane of an interlayer spacing of 7.17 Å. Consequently, the peak at $2(\theta)^0 = 12.35^0$ is taken as the reflection that accounts for pristine kaolinite interlayer space.

The peaks at the XRD diffraction pattern (not shown) for PRK, still appeared and remained the same as the main diffraction reflection for PIK when compared except for the appearance of a new peak at a lower $2\theta^0 = 7.849^0$. This is due to the expansion of the basal spacing and this increase in the interlayer space was the resultant effect of PVOH intercalation. This diffraction pattern which appeared at $2\theta^0 = 7.849^0$ is equivalent to the (001) basal planes with a spacing of $d_{001} = 11.23\text{Å}$ (1.123 nm), calculated to be equal to a lattice expansion of $(\Delta d) = 4.06\text{Å}$ (0.406 nm) (Table 4).

3.5 Adsorption Experiment

3.5.1. Effect of pH Variation

The effects of pH on the adsorption of BR2 and BG5 dyes by the adsorbents were investigated (Fig. 4 and 5). Therefore, there was a lesser quantity of the dyes (both BR2 and BG5) adsorbed in an acidic medium or at a lower pH.

Table 4: Basal interlayer space, d_{001} , and variation in space (Δd) of pristine and intercalated kaolinite

Sample	2θ	$D_{\text{spacing}} (\text{Å})$	$\Delta d (\text{Å})$
PRK	12.65	7.17	-
PIK	7.85	11.28	4.86

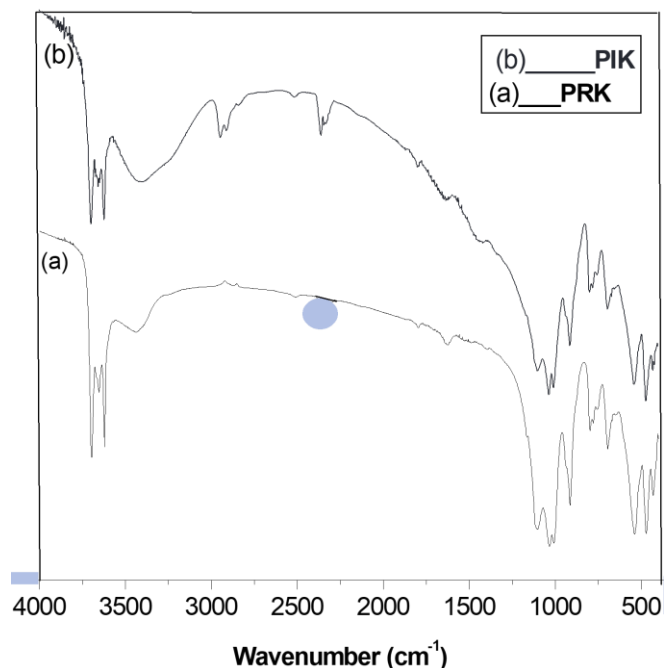


Fig. 3. FTIR spectra of (a) PRK and (b) PIK compared.

This implied that there was competition for the available negatively charged adsorption sites on the adsorbents between H⁺ ions (smaller ionic size) and the dye cations which could experience steric hindrance due to its bigger ionic and molecular size in solution (Bulutet *et al.*, 2008). Conversely, as the pH of the medium was gradually changed and transformed towards alkalinity or higher pH values, there was also a gradual increase in the adsorption capacities of the adsorbents (Fig. 4 and 5). This could be as a result of electrostatic attraction between the silanol (SiO⁻) negatively charged edges of the adsorbents at higher pH and the dyes ions in solution.

Therefore, the adsorptive response of PRK within the pH ranges studied showed an increase in percentage adsorption capacity from 24% to 99% for the removal of BR2 dye while it is from 7% to 97% for the removal of BG5 dye (Fig. 4). And for



PIK, it increased from 29% to 92% and from 54% to 75% for the removal of BR2 and BG5 dyes respectively, (Fig.5).

The graphical illustrations of the empirical study of the impact of the effect of adsorbent dose variation on dye uptake by PRK and PIK adsorbents are shown in Figure 6. The result showed that the sorption of both BR2 and BG5 dyes increases with the increase in both PRK and PIK adsorbent dosages (Adebowale *et al.*, 2014). This phenomenon has also been observed by many researchers (Gamze *et al.*, 2012; Adebowale *et al.*, 2014; Ogboduet *et al.*, 2015; Tahir *et al.*, 2016) and they have ascribed it to the availability of more adsorption sites and sufficiently large surface area. Though the increase in the number of dyes adsorbed is observed not to be linear to the corresponding adsorbent dose variation, yet the adsorption is proportional to each other.

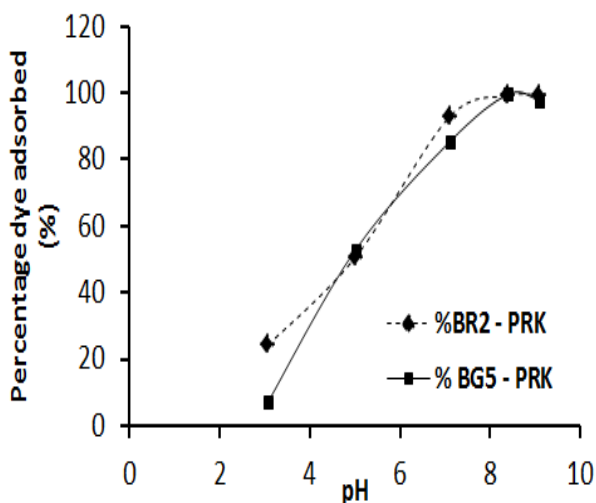


Fig. 4. Effect of pH on the adsorption capacity of PRK for the uptake of BR2 and BG5 dyes.

3.6 Adsorption equilibrium study

To optimize the design of an adsorption system to remove BR2 and BG5 dyes from the aqueous solution, five different equilibrium isotherm equations were used to model the experimental adsorption system. These are Langmuir and Freundlich (two parameter) isotherms; Redlich-Peterson (R-P) and Sips (three parameter) isotherms and Fritz-Schlunder (F-S) (four parameter) isotherm using non-linear regression curves (Fig. 7 and 8).

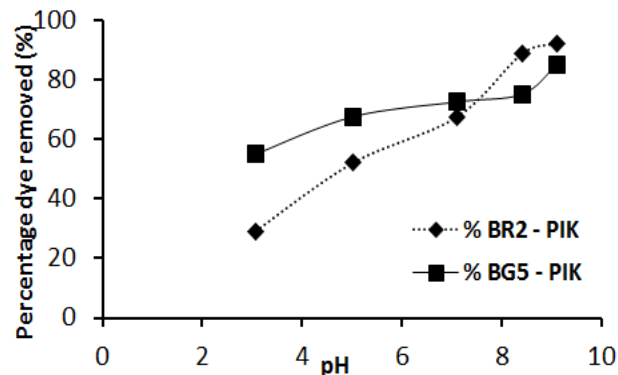


Fig. 5 Effect of pH on the adsorption capacity of PRK for the uptake of BR2 and BG5 dyes.

3.5.2. Effect of Adsorbent Dose Variation

An increase in the adsorbent dose from 0.02 to 0.15 g (Fig. 6), percentage dye adsorbed increased from 10.89 – 55.27% and 15.72 – 45.07% for the adsorption of BR2 onto PRK and PIK, respectively while percentage increments for the adsorption of BG5 unto PRK and PIK were from 28.32 to 78 55% and 39.88 to 61.11% respectively. The observed variation may be due to an increase in surface area, which led to an increase in the number of active adsorption sites (Sumanjit *et al.*, 2013; Dhaif-Allah *et al.*, 2019).

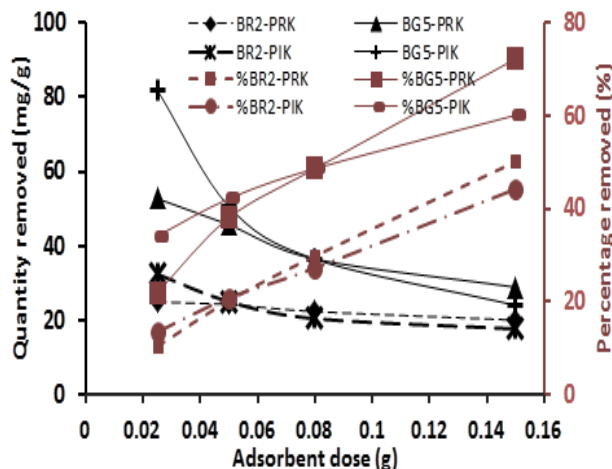


Fig. 6. PRK and PIK, adsorbent dose variation for the adsorption of BR2 and BG5 dyes.

Also, different statistical error function equations were applied to aid in judicious evaluation and appropriation of the right isotherm model equation for the adsorbents (Tables 6 and 7).

The observed high coefficient of determination (R^2) for the other isotherms are supported by the statistical error functions shown in Tables 6 and 7,



Redlich-Peterson isotherm model equation fitted the adsorption data for BR2 uptake onto PRK (Fig.8a), whereas BG5 dye uptake by the same adsorbent was best described by Fritz-Schulunder isotherm model equation (Fig.8b) (Jiaet al., 2017). The adsorption capacity of PRK for the uptake of BR2 and BG5 is 14.41 mg/g and 21.33 mg/g respectively (Table 5).

The adsorption data for BR2 uptake onto PIK best fitted the Sips isotherm (Fig.9a) while the adsorption of BG5 dye fitted the Fritz Schulunder isotherm (Fig.9b). The other isotherms showed that R² values were less than those obtained for the other models (Table 6).

Table 5 Adsorption Isotherm model parameters for the adsorption of BR2 and BG5

Model	Parameter	PRK		PIK	
		BR2	BR5	BR2	BR5
Langmuir	Q _{max} (mg/g)	14.41	21.33	24.02	41.649
	K _L (L/mg)	58.923	44.939	0.0684	0.0513
	R ²	0.8953	0.9630	0.9108	0.9717
Freundlich	K _F (L/mg)	6.970	10.083	5.639	9.732
	n _F	0.140	0.140	0.168	0.160
	R ²	0.8708	0.8804	0.9608	0.9183
Redlich-Peterson	K _{RP} (Lmg)	85.486	60.342	77.379	14.049
	a _{RP}	8.284	3.495	11.204	0.774
	β _{RP}	0.931	0.957	0.869	0.949
	R ²	0.9247	0.9729	0.9789	0.9752
Sips	Q _{ms} (mg/g)	17.691	21.796	29.311	42.201
	K _s (L/mg)	0.511	1.879	0.043	0.049
	n _s	0.381	0.748	0.467	0.939
	R ²	0.9036	0.9729	0.9825	0.9836
Fritz-Schuender	A _{FS}	9.335	0.9729	5.324	11.778
	α _{FS}	0.087	2.354	0.258	0.487
	BFS	20.514	16.042	0.033	0.311
	BFS	9.163	2.297	0.496	0.539
	R ²	0.6480	0.9843	0.9831	0.9844

Table 6: Criteria for the best fitted isotherm for the adsorption of BR2 and BG5 onto PRK

Criteria	BR2					BG5				
	La	Fr	R-P	Sips	FS	La	Fr	R-P	Sips	FS
R ²	0.895	0.871	0.925	0.904	0.648	0.963	0.880	0.973	0.973	0.984
ERRSQ	36.64	47.66	27.77	35.58	129.89	28.6	92.48	20.98	28.64	12.15
Var	4.83	5.96	3.97	5.08	21.65	3.57	11.56	3.01	4.09	2.03
(Error)										
HYBRID	118.75	375.34	124.23	201.28	59.42	63.72	560.87	57.36	69.51	53.24
MPSD	111.46	193.74	108.97	141.87	89.58	81.07	236.83	75.73	83.38	72.96
ARE	88.73	268.10	84.82	143.77	256.73	46.95	400.62	40.97	49.97	38.03
EABS	0.83	0.98	0.54	0.86	-17.89	-1.33	2.51	-1.01	-0.09	-3.13



Table 6: Criteria for the best fitted isotherm for the adsorption of BR2 and BG5 onto PIK

Criteria	BR2					BG5				
	La	Fr	R-P	Sips	FS	La	Fr	R-P	Sips	FS
R²	0.911	0.961	0.979	0.983	0.983	0.972	0.918	0.975	0.984	0.984
ERRSQ	28.89	12.71	6.84	5.66	5.47	25.55	73.80	22.38	14.79	14.09
Var	3.61	1.59	0.98	0.81	0.91	3.19	9.23	3.20	2.41	2.35
(Error)										
HYBRID	144.58	107.53	41.52	34.17	36.66	114.19	380.36	98.93	39.19	32.39
MPSD	120.24	103.70	64.43	58.43	60.54	106.86	195.03	99.46	62.60	56.91
ARE	103.27	76.81	29.66	24.20	26.18	81.57	271.69	70.66	27.99	23.13
EABS	-7.35	1.13	-0.23	0.06	0.12	-5.39	3.11	-4.35	-1.18	0.66

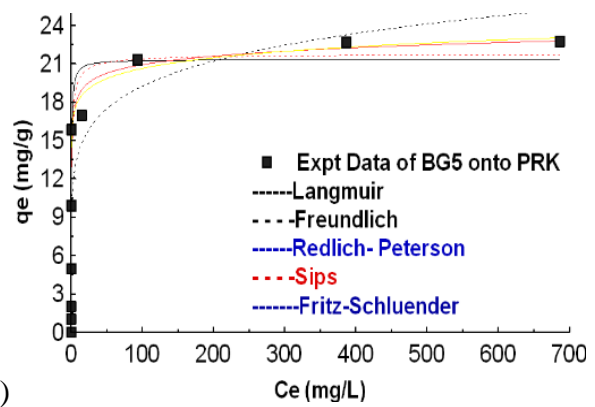
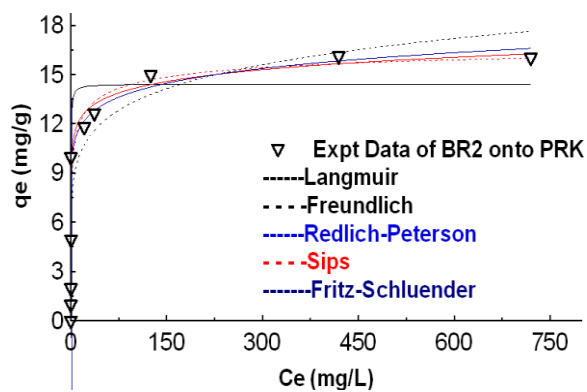


Fig. 7. Non-linear adsorption Isotherm regression plot for the adsorption of (a) BR2 and (b) BG5 dye onto PRK.

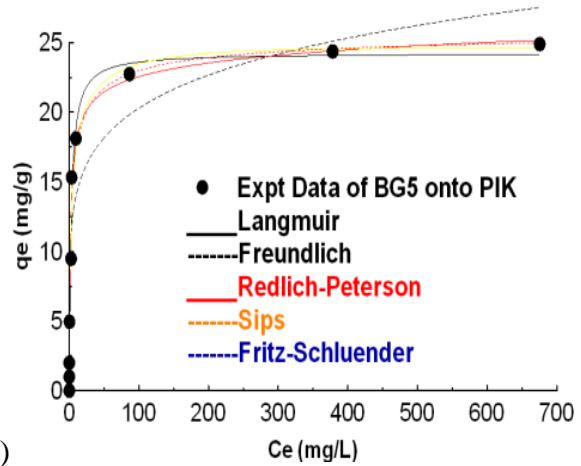
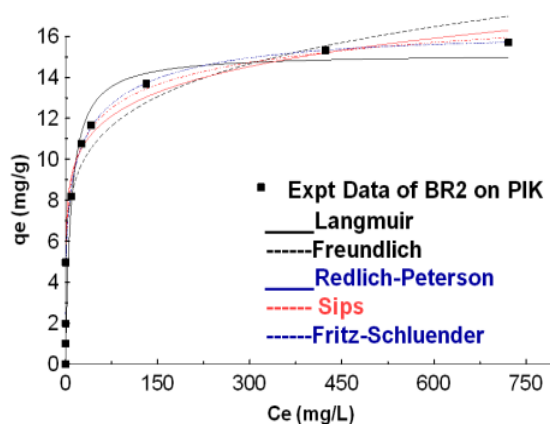


Fig. 8. Non-linear adsorption Isotherm regression plot for the adsorption of (a) BR2 and (b) BG5 dye onto PIK

3.7 Adsorption Kinetics

Three pseudo-first order (PFOM), pseudo-second order (PSOM) and Elovich kinetic model (EKM) were used to explain the adsorption mechanism of the adsorption of BR2 and BG5 dyes unto PRK and

PIK using nonlinear regression plots (curves not shown). Three error deviation functions were employed to support the correlation based criterion for the determination of the best fit model as shown in Table 8.



The non-linear fitting of EKM equation compared to PFOM and PSOM kinetic equations at different solution concentrations gave the highest value of the coefficient of determination (R^2). Therefore, the agreement of adsorption data and the Elovich model showed better improvement. (Table 8), which also agreed with the outcome of statistical error analysis (Wu *et al.*, 2009 Inyinboret *al.*, 2017).

The EKM parameter (β) which indicates the extent of surface coverage seems to increase proportionally with the initial dye concentrations (Table 8), such that the initial dye concentration increased from 20 to 100 mg/L the surface coverage (β) of the BR2 and BG5 onto PRK and PIK also increased (Balsamo *et al.*, 2013; Shieuet *al.*, 2017).

Table 8: Criteria and comparison of bed fitted out of the three kinetic modes for the adsorption of dyes

	PRK				PIK			
	BR2		BG5		BR2		BG5	
	20 mg/L	50 mg/L	20 mg/L	50 mg/L	20 mg/L	50 mg/L	20 mg/L	50 mg/L
EloVich parameters								
α mg/(g.min)	0.58	0.97	0.93	1.10	2.98	1.33	1.96	1.57
β (g/mg) x 10 ²	71.52	8.30	5.85	9.97	1.39	2.47	2.87	6.59
R ²	0.971	0.962	0.915	0.993	0.963	0.947	0.942	0.885
SSE	3.73	7.36	15.69	2.02	1.79	6.54	13.94	9.23
Var	0.34	0.67	1.43	0.18	0.16	0.59	0.30	0.84
RMSE	0.61	0.86	1.25	0.45	0.43	0.76	0.58	0.96
Pseudo first order kinetic parameters								
qe (mg/g)	9.10	12.13	9.45	15.84	7.10	9.70	6.54	6.99
K ₁ (min ⁻¹)	4.55	8.19	5.14	26.98	44.72	8.57	11.57	11.51
R ²	0.871	0.908	0.862	0.797	0.927	0.935	0.618	0.551
SSE	16.87	18.00	22.80	57.95	3.56	8.13	20.19	35.93
Var	1.53	1.64	2.07	5.27	0.32	0.74	1.84	3.27
RMSE	1.30	1.34	1.51	2.41	0.90	0.81	1.42	1.90
Pseudoseond order kinetic parameters								
qe (mg/g)	9.54	12.62	9.99	16.77	6.94	7.24	6.77	7.33
K ₂ (g/mg.min)	0.64	0.98	0.62	2.21	11.31	1.38	3.33	3.03
h (mg/g min)	58.4	155.3	62.6	620.1	593.0	198.2	139.1	128.1
R ²	0.942	0.961	0.905	0.903	0.963	0.888	0.757	0.652
SSE	7.62	7.65	22.80	27.85	1.82	13.85	3.32	27.90
Var	0.69	0.70	2.07	2.53	0.17	1.26	1.27	2.54
RMSE	0.87	0.87	1.67	1.67	0.42	1.18	1.18	1.67

3.8 Adsorption Thermodynamics

The thermodynamic parameters associated with the adsorption, namely; free energy (ΔG^0), enthalpy (ΔH^0) and entropy (ΔS^0) were studied at four different temperatures as shown in Table 9. The evaluation of the effect of temperature on the sorption of the dyes onto PRK and PIK adsorbents was carried out by calculations using Eqns. 3, 4 and 5. The equilibrium partition constant (k_d) value was made dimensionless by applying Slobodan

specification by using the following equations (Slobodan 2007);

$$k_d = \frac{C_A}{C_S} \tag{3}$$

$$\Delta G^0 = -RT \ln(1000)k_d \tag{4}$$

$$\ln k_d = \frac{\Delta S^0}{R} - \frac{\Delta H^0}{RT} \tag{5}$$

where K_d is the equilibrium partition constant (dimensionless), C_A and C_S are respectively the concentration of BR2 and BG5 adsorbed on the



adsorbent and the ones left in the solution at equilibrium (mg/L), T is the temperature (K) of the system and R is the gas constant (8.314 J/mol.K). The values of ΔH^0 and ΔS^0 in equation [5] were respectively calculated from the slope and intercept of plots of ΔG^0 versus T .

Table 9 shows that values of ΔG^0 were negative and reveal that the adsorption is spontaneous and seems to tend to be more spontaneous with an increase in temperature (Table 9).

The positive value for the enthalpy change, ΔH^0 , implied that the adsorption process is endothermic. The negative values obtained for changes in the entropy of adsorption ΔS^0 (Table 9) are consequences of decreasing the degree of randomness or increasing orderliness (Table 9). Consequently, it is an indication that the adsorption process is irreversible.

Table 9: Thermodynamic parameters for the adsorption of BR2 and BG5 dyes by intercalated adsorbents

Adsorbent	Adsorbate	ΔG^0 (KJ/mol.)				ΔH^0 (KJ/mol)	ΔS^0 (J/mol./K)
		303 K	308 K	313 K	323 K		
PRK	BR2	-21.98	-22.52	-23.54	-24.44	16.13	-0.125
PRK	BG5	-23.65	-24.08	-24.59	-25.67	7.23	-0.101
PIK	BR2	-20.51	-20.94	-21.34	-22.99	17.41	-0.124
PIK	BG5	-20.70	-21.20	-21.62	-22.83	11.66	-0.106

3.9 Desorption study

The desorption efficiencies when 0.5% of 0.02 M H_2SO_4 , HCl, CH_3COOH , NaCl and NaOH were used are indicative in Fig. 9. which shows that the highest dye desorption was achieved by using CH_3COOH and HCl solutions. The outcomes are above 94% and 63% (CH_3COOH) and 71% and 39% (HCl) for BR2 and BG5 dyes respectively from PRK while 76% and 57% (CH_3COOH) and about 54% and 74% (HCl) of BR2 and BG5 respectively from PIK (Fig. 9a and 9b). According to Ahmad and Kumar, (2010) and Inyinborae *et al*

(2015), If desorption is attained at the water/neutral pH, it means that the dye is weakly adsorbed to the adsorbent surface, but If the dye desorption is induced by sulphuric/hydrochloric acid or by an alkaline, the adsorption by ion exchange, but if it is driven by organic acids, such as acetic acid, the dye may be chemisorbed to the adsorbent. that Therefore, the effectiveness of desorption of BR2 and BG5 dyes by acidic solutions (CH_3COOH and HCl) is because the adsorption, is probably dominated by Coulombic interaction and chemisorption (Ahmad and Kumar, 2010).

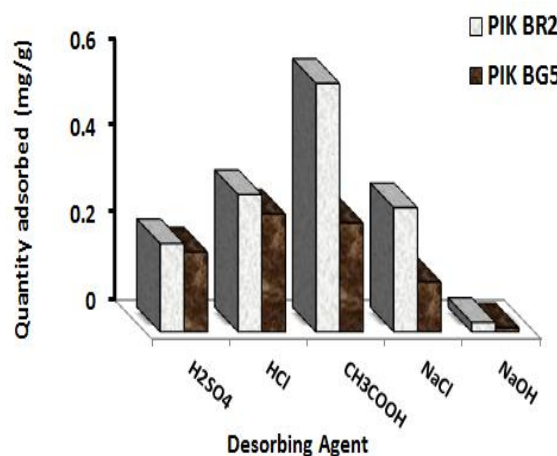
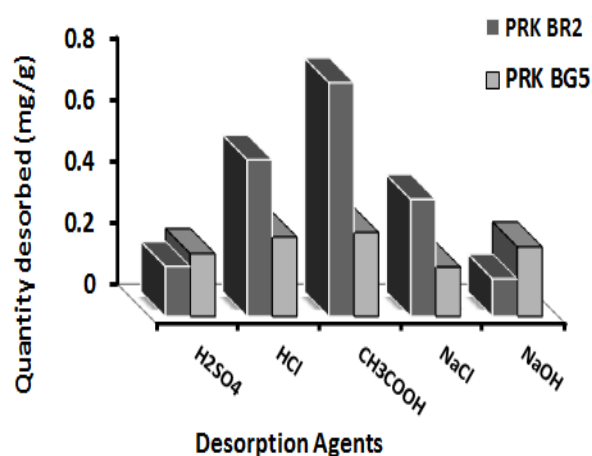


Figure 9: Desorption of BR2 and BG5 dyes by different desorbing agents from PRK and PIK adsorbents



4.0 Conclusion

Purified raw kaolinite (PRK) clay was successfully intercalated with PVOH by a direct method. The PVOH intercalated kaolinite (PIK) has a higher adsorption capacity than PRK do. This can be explained by the resultant effect of better specific surface area and higher cation exchange capacity instigated by intercalation. Out of the three kinetic models used, the Elovich equation showed a better fit and predicted chemisorption for both adsorbent interactions with BR2 and BG5 dyes. The use of ΔH^0 , ΔG^0 and ΔS^0 thermodynamic parameters to study the effect of temperature on the adsorption process revealed that the adsorption rates increased with an increase in temperature. Moreover, the adsorption of BR2 and BG5 dyes onto both adsorbents were spontaneous, endothermic and with increased randomness on the surfaces of the adsorbents with regards to the negative values of ΔG^0 , the positive values of ΔH^0 and positive values of ΔS^0 , respectively. CH_3COOH was effective for the desorption of the dyes from the two adsorbents.

5.0 Reference

- Abdullahi T., Harun Z. and Othman M. H. D. (2017). A review on sustainable synthesis of zeolite from kaolinite resources via hydrothermal process. *Advanced Powder Technology*, 28, 8, pp 1827-1840, <https://doi.org/10.1016/j.apt.2017.04.028>.
- Abella, S. R. and Zimmer, B. W. (2007). Estimating organic carbon from loss-on-ignition in northern Arizona forest soils. *Soil Science Society of America Journal*. 71, pp. 545–550.
- Adebowale, K. O., Olu-Owolabi, B. I., Chigbundu, E. C. (2014). Removal of Safranin-O from aqueous solution by adsorption onto kaolinite clay. *Journal of Encapsulation and Adsorption Sciences*. 4, pp. 89-104. <http://dx.doi.org/10.4236/jeas.2014.43010>
- Adejumoke A. I., Folahan A. A. and Gabriel A. (2015). Adsorption of Rhodamine B Dye from Aqueous Solution on Irvin giagabonensis Biomass: Kinetics and Thermodynamics Studies. *South African Journal of Chemistry*. 68, pp. 115–125
- Ahmad, R. and Kumar, R. (2010). Adsorptive removal of Congo red dye from aqueous solution using bael shell carbon. *Applied Surface Science*. 257, pp. 1628–1633.
- Tabak A., Afsin B., Caglar B. and Caglar S. 2016. dimethyl Sulfoxide Species Entrapped by Raw and Acid-Activated Sepiolite Framework. *Sinop University Journal of Natural Sciences*. 1, 1, pp. 76 – 82.
- AL Da,amy M.A. AL Rubaeey, E.T. AL Khaleeli, A.B. Abdul Majeed, M.N. and AL Njar Z.A. (2013) Adsorption of cationic dyes from synthetic textile effluent by Iraqi porcelanite rocks, *Journal of Asian Scientific Research*, 3, 10. pp. 1011-1021.
- Alkan, M., Benlikaya, R., (2009). Poly (vinyl alcohol) Nanocomposites with sepiolite and heat-treated Sepiolites. *Journal of Applied Polymer Science*. 112, pp. 3764–3774. DOI 10.1002/app.29830
- Bahareh A. E., Banafsheh A. E., Mina S. K, and Seyyedeh Z.G. (2014). Industrial wastewater treatment by membrane systems. *Indian Journal of Fundamental and Applied Life Sciences*. 4, pp. 1168-1177
- Balázs Z., Erzsébet H., Éva M., Róbert K, and János. (2015). Preparation and characterization of kaolinite nanostructures: reaction pathways, morphology and structural order. *Clay Minerals*. 50, pp. 329–340
- Balsamo, M., Budinova, T., Erto, A.; Lancia, A., Petrova, B., Petrov, N., Tsyntsarski, B. (2013). CO₂ adsorption onto synthetic activated carbon: Kinetic, thermodynamic and regeneration studies. *Separation and Purification Technology*. 116, pp. 214–221.
- Bello O. S., Adeogun I. A., Ajaelu J. C. and Fehintola E. O. (2008). Adsorption of methylene blue onto activated carbon derived from periwinkle shells: kinetics and equilibrium studies. *Journal of Chemical Ecology*. 24, 4, pp. 285–295
- Saikia B. J. and Parthasarathy G. K. (2010). Fourier Transform Infrared Spectroscopic Characterization of Kaolinite from Assam and Meghalaya. *Northeastern India. Journal of Modern Physics*. 1, pp. 206-210. Doi:10.4236/jmp.2010.14031
- Bhattacharyya K. G, Sen G. S., and Sarma G. K. (2014). Interactions of the dye, Rhodamine B



- with kaolinite and montmorillonite in water. *Applied Clay Science* 99, pp. 7–17.
- Bulut, E., Ozacar, M., and Sengil, I. A. (2008). Adsorption of Malachite Green Onto Bentonite: Equilibrium and Kinetic Studies and Process Design. *Microporous and Mesoporous Materials*. 115, pp. 234–246.
- Carretero, M. I. and Pozo, M. (2010). Clay and non-clay minerals in the pharmaceutical and cosmetic industries part II. Active ingredients. *Applied Clay Science*. 47, (3–4), pp. 171–181.
- Dewi, R. Agusnar, H. Alfian, Z. Tamrin (2018). Characterization of technical kaolin using XRF, SEM, XRD, FTIR and its potentials as industrial raw materials *Journal of Physics: Conference Series* 1116 pp. 042010 IOP Publishing doi:10.1088/1742-6596/1116/4/042010
- Dhaif-Allah M. A. H., Taqui S. N., Syed U. T., and Syed A. A. (2019). Development of sustainable acid blue 113 dye adsorption system using nutraceutical industrial Tribulusterrestris spent. *SN Applied Sciences*. 1, (4), pp. 330
- Dias, M., Valério, A., de Oliveira, D., de Souza, A. A. and de Souza, S. M. U. (2020). Adsorption of natural annatto dye by kaolin: kinetic and equilibrium, *Environmental Technology*, 41, 20, pp. 2648-2656.
- Donat R., Akdogan A., Erdem E. Cetisli H. 2005. Thermodynamics of Pb^{2+} and Ni^{2+} adsorption onto natural bentonite from aqueous solutions. *Journal of Colloid and Interface Science*. 286, 1, pp. 43-52.
- Eddy, N. O., Udoh, C. O. and Ukpong, I. J. (2004). Heavy metals in the sediment of the Cross River Estuary at Oron, South Eastern Nigeria. *African Journal of Environmental Pollution and Health*, 3, 1, pp. 6-10
- El Bakouri, H., Usero, J., Morillo, J., and Ouassini, A., (2009). Adsorptive features of acid-treated olive stones for drin pesticides: equilibrium, kinetic and thermodynamic modeling studies. *Bioresources Technology*. 100, pp. 4147–4155.
- Unuabonah E. I., Ugwuja C. G., Omorogie M. O., Adewuyi A. and Oladoja N. A. (2018). Clays for Efficient Disinfection of Bacteria in Water. *Applied Clay Science*. 151, pp. 211- 223. <http://dx.doi.org/10.1016/j.clay.2017.10.005>
- Feng-Chin W., Ru-Ling T. and Ruey-Shin J. (2009). Characteristics of Elovich Equation Used for the Analysis of Adsorption Kinetics in Dye–Chitosan Systems. *Chemical Engineering Journal* 150, (2-3), pp. 366-373, DOI: 10.1016/j.cej.2009.01.014
- Freundlich, H.M.F. 1906. *Journal of Physical Chemistry*. Pp. 385–370.
- Nwosu F. O., Ajala O. J., Owoyemi R. M. and Raheem B. G. (2018). Preparation and characterization of adsorbents derived from bentonite and kaolin clays. *Applied Water Science*. 8, pp. 195 – 205, <https://doi.org/10.1007/s13201-018-0827-2>
- Fritz W., Schluender E. U. (1974). *Chemical Engineering Science*, 29, 5, pp. 1279 – 1282.
- Gamze V., Ahmet D., Kaan Y., Selin T., Elif S. and Sinan B. M. 2012. Removal of 4-nitrophenol from aqueous solution by natural low cost adsorbents (using Zeolite and Bentonite). *Indian Journal of Chemical Technology*. 19, pp. 7-25.
- Gardolinski J. E, Peralta-Zamora P, and Wypych F. (1999). Preparation and Characterization of a Kaolinite-1-methyl-2-Pyrrolidone Intercalation Compound. *Journal of Colloid and Interface Science*. 211, (1), pp. 137 - 141. doi: 10.1006/jcis.1998.5982.PMID: 9929445
- Havelcova, T. H. M., Mizera, J., Sykorov̇ia, I., Pekar, M., (2009). Sorption of metal ions on lignite and the derived humic substances. *Journal of Hazardous Materials*. 161, pp. 559–564.
- Herney-Ramirez, J., Vicente, M. A., and Madeira, L. M., (2010). Heterogeneous photo-Fenton oxidation with pillared clay based catalysts for wastewater treatment: a review. *Applied Catalysis B: Environmental*. 98, pp. 10–26.
- Ho, Y., McKay, G. A. (1998). Comparison of chemisorption kinetic models applied to pollutant removal on various sorbents. *Process Safety and Environmental Protection*. 76, pp. 332-340.
- IFRA Analytical Method (2019). Determination of peroxide value ‘ISO-Standard 3960’ modified 3rded 2001 AOCS CD 8b-90 *European Pharmacopeia Leatherhead Food R. A. Geneva, Switzerland*.
- Inyinbor A. A, Adekola F. A. and Olatunji G. A. (2017). Liquid phase adsorptions of Rhodamine



- B dye onto raw and chitosan supported mesoporous adsorbents: isotherms and kinetics studies. *Applied Water Science*. 7, pp. 2297–2307 DOI 10.1007/s13201-016-0405-4
- Jia, Z., Li, Z., Ni, T., and Li, S. (2017). Adsorption of low-cost absorption materials based on biomass (*Cortaderiaselloana* flower spikes) for dye removal: Kinetics, isotherms and thermodynamic studies. *Journal of Molecular Liquids*. 229, pp. 285–292.
- Jin, L. Liu, Q. Sun, Z. Ni, X. and Wei, M. (2010). Preparation of 5-fluorouracil/ β -cyclodextrin complex intercalated in layered double hydroxide and the controlled drug release properties, *Industrial and Engineering Chemistry Research*. 49, pp. 11176–11181.
- Lagergren, S., (1898). About the theory of so called adsorption of soluble substances, (translated)-*The Royal Swedish Academy of Sciences' Documents*. 24, pp.1-39.
- Langmuir, I. (1918). *Journal of the American Chemical Society*. 40, 9, pp. 1361–1403.
- Letaief S. and Detellier C. (2008). Interlayer grafting of glycidol (2, 3-epoxy-1-propanol) on kaolinite. *Canadian Journal of Chemistry*, 86, pp. 1-6
- Low, M. J. D. (1960). Kinetics of chemisorption of gases on solids. *Chemical Reviews*. 60, pp. 267–312.
- Ma, X., Zhou, W., Fu, Z., Cheng, Y., Min, M., Liu, Y., Zhang, Y., Chen, P., Ruan, R., (2014). Effect of wastewater-borne bacteria on algal growth and nutrients removal in wastewater-based algae cultivation system. *Bioresource Technology*. 167, pp. 8–13.
- Makó, E.; Kovács, A.; Kristóf, T. (2019). Influencing parameters of direct homogenization intercalation of kaolinite with urea, dimethyl sulfoxide, formamide, and N-methylformamide. *Applied Clay Science*. 182, pp. 105- 287
- Makó, E., Kristóf, J., Horváth, E. and Vágvölgyi, V. (2013). Mechanochemical intercalation of low reactivity kaolinite. *Applied Clay Science*. 83–84, pp. 24–31.
- Mbaye, A., Diop, C. A. K., Mieke B. J., Senocq F. and Maury F., 2014. Characterization of natural and chemically modified kaolinite from Mako (Senegal) to remove lead from aqueous solutions. *Clay Minerals*. 49, (n° 4), pp. 527-539. ISSN 0009-8558.
- Mbey, J. A., Thomas, F., Ngally S. C. J., Liboum; N. D. (2013). An insight on the weakening of the interlayer bonds in a Cameroonian kaolinite through DMSO intercalation. *Applied Clay Science*. 83–84, pp. 327–335.
- Meziane O., Bensedira A., Guessoum M. and Haddaoui N. 2017. Preparation and Characterization of Intercalated kaolinite with urea, dimethyl formamide and an Alkylammonium Salt Using Guest Displacement Reaction. *Journal of Materials and Environmental Sciences*. JMES. 8 .10, pp. 3625-3635
- El-Latif M. M. A., Elkady M. F., Ibrahim A. M., and Mona O. (2010). Alginate/ Polyvinyl Alcohol - Kaolin Composite for Removal of Methylene Blue from Aqueous Solution in a Batch Stirred Tank Reactor. *Journal of American Science*. 6, 5, pp. 12- 34
- Nandi, B. K., Goswami, A. and Purkait, M. K. (2009). Adsorption characteristics of brilliant green dye on kaolin. *Journal of Hazardous Materials*, 161, 1, pp. 387-395. <https://doi.org/10.1016/j.jhazmat.2008.03.110>
- Caponi N., Collazzo G. C., Jahn S. L., Dotto G. L., Mazutti M. A., and Foletto E. L. (2017). Use of Brazilian Kaolin as a Potential Low-cost Adsorbent for the Removal of Malachite Green from Colored Effluents. *Materials Research*. 20, (2), pp. 1 -13 <http://dx.doi.org/10.1590/1980-5373-mr-2016-0673->
- Odoemelam, S. A., Emeh, N. U. and Eddy, N. O. (2018). Experimental and computational Chemistry studies on the removal of methylene blue and malachite green dyes from aqueous solution by neem (*Azadirachthaindica*) leaves. *Journal of Taibah University of Science*, 12, 3, pp. 255–265doi.org/10.1080/16583655.2018.-1465725.
- Ogbodu, R. O., Omorogie, M. O., Unuabonah, E. I., and Babalola, J. O. (2015). Biosorption of heavy metals from aqueous solutions *Parkiabiglobosa* biomass: equilibrium, kinetics, and thermodynamic studies. *Environmental Progress and Sustainable Energy*. 34, 6, pp. 1694–1704.



- Omorogie, M. O., Babalola, J. O., Unuabonah, E. I., Gong, J. R. (2014). Hybrid materials from agro-waste and nanoparticles: implications on the kinetics of the adsorption of inorganic pollutants. *Environmental Technology*. 35, 5, pp. 611–619.
- Djomgoue P. and Njopwouo D. (2013). FT-IR Spectroscopy Applied for Surface Clays Characterization. *Journal of Surface Engineered Materials and Advanced Technology*. 3, pp. 275–282
<http://dx.doi.org/10.4236/jsemat.2013.34037>
- Rashid, A., Bhatti, H. N., Iqbal, M., and Noreen, S. (2016). Fungal biomass composite with bentonite efficiency for Nickel and Zinc adsorption: a mechanistic study. *Journal of Ecological Engineering*. 91, pp. 459–471,
- Redlich, O. Peterson, D. L. 1959. *The Journal of Physical Chemistry* 63, 6, pp. 1024–1024.
- Salwa D. A. and Essam H. (2011). Characterization of Egyptian Smectitic Clay Deposits by Methylene Blue Adsorption. *American Journal of Applied Sciences*. 8, 12, pp. 1282–1286, ISSN 1546-9239
- Sarma, G. K., Sen G. S. and Bhattacharyya K.G. (2019). Removal of hazardous basic dyes from -aqueous solution by adsorption onto kaolinite and acid-treated kaolinite: kinetics, isotherm and mechanistic study. *SN Applied Sciences* 1, pp. 211 |<https://doi.org/10.1007/s42452-019-0216-y>
- Shaban, M. Sayed, M. I. Shahien, M. G. Abukhadra, M. R. Ahmed, Z. M. (2018). Adsorption behavior of inorganic and organic modified kaolinite for Congo red dye from water; kinetic modeling and equilibrium studies. *Journal of Sol-Gel Science and Technology*. 87, pp. 427–441.
- Shieu, A., Hu, S. C., Chang, S. M., Ko, T. Y., Hsieh, A., Chan, A. 2017. Adsorption kinetics and breakthrough of carbon dioxide for the chemical modified activated carbon filter used in the building. *Sustainability*. 9, pp. 1533.
- Sips R. (1948). Combined form of Langmuir and Freundlich equations. *The Journal of Chemical Physics*. 16, pp. 490–495.
- Slobodan, K. Milonjic, (2007). A consideration of the correct calculation of thermodynamic parameters of adsorption. I. 72, (12), pp. 1363–1367
- Sousa J. P., Splendor D., Gonçalves I. M. B., Costa P., and Sousa L. J. M. (2013). Note on the Measurement of Bulk Density and Tapped Density of Powders According to the *European Pharmacopeia*. 143, pp. 1098–1100. doi: 10.1208/s12249-013-9994-5
- Sumanjit K., Rani S., and Mahajan R. K. (2013). Adsorption Kinetics for the Removal of Hazardous Dye Congo Red by Biowaste Materials as Adsorbents. *Journal of Chemistry*, Article ID 628582, 12pp. <https://doi.org/10.1155/2013/628582>
- Tahir, M. A., Bhatti, H. N., and Iqbal, M. (2016). Solar red and brittle blue direct dyes adsorption onto Eucalyptus angophoroides bark: equilibrium, kinetics and thermodynamic studies. *Journal of Environmental Chemical Engineering*. 4, pp. 2431–2439.
- Tan, D. Yuan, P. Annabi-Bergaya, F. Dong, F. Liu, D. and He, H. (2015). A comparative study of tubular halloysite and platy kaolinite as carriers for the loading and release of the herbicide amitrole. *Applied Clay Science*. 114, pp. 190–196.
- Unuabonah, E. I., Olu-Owolabi, B. I., Adebowale, K. O., Yang, L. Z. (2008). Removal of Lead and Cadmium from Aqueous Solution by Polyvinyl Alcohol-Modified Kaolinite Clay: A Novel Nano-Clay Adsorbent. *Adsorption Science and Technology*, 26, pp. 383–405. <http://dx.doi.org/10.1260/02636174.26.6.383>
- Vučurović V. M., Razmovski R. N., Tekić and M. N., (2012). Methylene blue (cationic dye) adsorption onto sugar beet pulp: equilibrium isotherm and kinetic studies. *Journal of the Taiwan Institute of Chemical Engineers*. 43, (1), pp. 108–111.
- Wang, T. H., Li, M. H., and Teng, S. P. (2009). Bridging the gap between batch and column experiments: a case study of Cs adsorption on granite. *Journal of Hazardous Materials*. 161, pp. 409–415.
- Xue, M. Q., Li, J., and Xu, Z. M., (2012). Environmental friendly crush-magnetic separation technology for recycling metal-plated plastics from end-of-life vehicles. *Environmental Science and Technology*. 46, pp. 2661–2667.



- Kuang Y., Zhang X. and Zhou S. (2020). Adsorption of Methylene Blue in Water onto Activated Carbon by Surfactant Modification. *Water*. 12, pp. 587; doi:10.3390/w12020587
- Zhang S. H, Zhou Y. C, Ou X. M, Qiang Y. H, Xia H. Guang P. X., Yu G. and Pu F. X. (2013). Study on the occurrence status of formamide in kaolinite-formamide intercalation system and the microstructure of its compounds by FTIR and XRD. *Spectroscopy and Spectral Analysis*. 33, 11, pp. 2978-2982.

Conflict of Interest

The authors declared no conflict of interest.

